

GROWTH AND MAGNETIC STRUCTURE OF $\text{La}_{0.67}\text{Sr}_{0.33}\text{MnO}_3$ FILMS

G.W. BROWN, Q.X. JIA, E.J. PETERSON, D.K. HRISTOVA, M.F. HUNDLEY,
J.D. THOMPSON, C.J. MAGGIORE, J. TESMER, and M.E. HAWLEY
Los Alamos National Laboratory, Los Alamos, NM 87545, hawley@lanl.gov

LA-UR--97-1502
CONF-970302-21

ABSTRACT

Growth of LaMnO_3 films that exhibit colossal magnetoresistance (CMR) has concentrated heavily on Ca doped materials. However, since the 33% Sr doped films are ferromagnetic at room temperature, they are ideal candidates for dual growth-magnetic structure studies using scanned probe techniques. In this study, interest was focused on the relations between growth/processing parameters, film morphology, and electronic/magnetic properties. In addition, films were grown on both LaAlO_3 (LAO) and SrTiO_3 (STO) to examine the results of stress induced by different substrate mismatches. $\text{La}_{0.67}\text{Sr}_{0.33}\text{MnO}_3$ (LSMO) was grown using pulsed laser deposition (PLD) at temperatures between 500 °C and 800 °C. The film microstructure, crystallinity, and magnetic and electrical properties were characterized by room temperature scanning tunneling microscopy (STM), atomic force microscopy (AFM), magnetic force microscopy (MFM), x-ray diffraction, and temperature dependent transport and magnetization measurements. The growth trends follow those previously reported for Ca doped films. Grains increase in size with increasing temperature and coalesce into extended layers after annealing. Although topographic contributions complicate interpretation of some MFM data, local magnetic structure observed here is generally associated with film defects.

INTRODUCTION

There has been increasing interest in the deposition of $\text{La}_{1-x}\text{A}_x\text{MnO}_3$ ($\text{A} = \text{Ca}, \text{Sr}, \text{Ba}$) thin films due to the potential application of their CMR in magnetic sensing technologies. The $x = 0.33$ Sr doped film is especially interesting since it has a critical temperature (T_c) of ~380 K and is ferromagnetic at room temperature [1]. It is therefore suited to a wide variety of analytical techniques including magnetic force microscopy. Several groups have grown LSMO with PLD [2,3] but few growth parameters were examined. In this study, we examine the effect of different deposition parameters on LSMO topographic and magnetic microstructure and search for correlations with transport and magnetization measurements.

EXPERIMENT

LSMO films were grown at substrate temperatures of 500 °C, 650 °C and 800 °C on LaAlO_3 (LAO) and SrTiO_3 (STO) substrates using a XeCl laser (308 nm) incident on a stoichiometric target. Pulses of 20 nsec duration and 2 J/cm^2 energy were used at 5 Hz in 200 mTorr of oxygen. Film thicknesses of ~1300 Å were measured by Rutherford backscattering spectroscopy (RBS). In order to achieve uniform sample preparation and more reliably compare the effects of different processing parameters, all substrates were cut from a single crystal wafer of each material and films were grown simultaneously on both types of material. In addition, two pieces of each substrate were used in each deposition run to allow comparison of as-deposited and annealed films. Finally, after all of the depositions were completed, the films to be heat-treated were taken as a group and annealed simultaneously in single boat in one furnace cycle.

All of the films were characterized with STM, AFM, and MFM to determine their topographic and magnetic microstructure. Typical STM tunneling parameters were 1.5 V tip bias at 70 pA while AFM/MFM was carried out in tapping/lift mode [4] with high-coercivity cobalt-chrome coated Si tips on Si cantilevers. MFM and AFM scans are interleaved during data acquisition so that the magnetic features could be correlated directly with surface structure. All microscopies were done in the ambient laboratory atmosphere. X-ray diffraction and temperature-dependent four-point resistivity measurements were also made on all of the films

DISTRIBUTION OF THIS DOCUMENT IS UNLIMITED. 

MASTER

DISCLAIMER

This report was prepared as an account of work sponsored by an agency of the United States Government. Neither the United States Government nor any agency thereof, nor any of their employees, make any warranty, express or implied, or assumes any legal liability or responsibility for the accuracy, completeness, or usefulness of any information, apparatus, product, or process disclosed, or represents that its use would not infringe privately owned rights. Reference herein to any specific commercial product, process, or service by trade name, trademark, manufacturer, or otherwise does not necessarily constitute or imply its endorsement, recommendation, or favoring by the United States Government or any agency thereof. The views and opinions of authors expressed herein do not necessarily state or reflect those of the United States Government or any agency thereof.

DISCLAIMER

**Portions of this document may be illegible
in electronic image products. Images are
produced from the best available original
document.**

and magnetization normal to the surface (in 100 Oe applied field) was examined on the annealed films. Film stoichiometry was checked with Rutherford backscattering analysis.

RESULTS

X-ray diffraction showed substrate lattice parameters in agreement with published values and a $\sim 0.5^\circ$ miscut of the STO. The deposited LSMO appeared epitaxial in the growth direction at all three temperatures with lattice parameters normal to the surface shown in Table I. There is no obvious correlation with deposition temperature but there was a shortening of this parameter with annealing in 5 of the 6 films. In general, the 650 °C and 800 °C films deposited on LAO had lattice parameters normal to the surface that were longer than bulk LSMO (3.86 Å), which is the expected response to the compressive stress exerted by the lattice mismatch between LAO and LSMO (see Table 1). The situation for the higher temperature depositions on STO is not as clear. At 650 °C, the lattice parameter normal to the surface is contracted (STO should exert tensile stress on LSMO), but the 800 °C film shows the opposite response. As a group, the annealed 500 °C depositions on both substrates had lattice constants closest to the bulk value.

While it was possible to extract lattice parameters from the x-ray scans, the peaks were broad, indicating possible inhomogeneity in the samples. This was also implied by wide transitions in the transport and magnetization measurements shown in Figure 1. All of the films show a metal-insulator transition coinciding with the drop in magnetization which is the general behavior of these CMR films. As seen in the 800 °C deposition on STO, even anomalies in the resistivity peak are mirrored in the magnetization, reflecting the link between the two. Unfortunately, the transitions on all films occur at lower than expected temperatures (particularly on STO), indicating a T_c below 300 K. This is unexpected since the RBS showed stoichiometry reasonably close to the expected value on two representative samples.

STM and AFM images of the films as-deposited on LAO are shown in the left panels of Figure 2 and follow very closely the results of previous studies on Ca doped films [5]. The results from deposition on STO were virtually identical with no indication of substrate-induced strain in the as-deposited films. At 800 °C and 650 °C there are very smooth films with RMS roughnesses/grain sizes of 9Å/35nm and 13Å/20nm respectively. At 500 °C however, there is clustering that is characteristic of low mobility and resulting 3 dimensional growth leading to a roughness of ~ 75 Å. Grain size continues to follow the trend as close inspection shows that the clustering grains are ~ 15 nm across. On STO we find roughness/grain sizes of 9Å/44nm, 13Å/21nm, and 89Å/16nm for the 800 °C, 650 °C and 500 °C depositions respectively.

Annealing produces the structures shown in the right panels of Figure 2. Common features are faceting and screw dislocations with unit cell Burger's vectors. The 650 °C and 800 °C films also show pinholes near the terrace edges while the 500 °C films show much larger voids distributed across the surface. These features will be clearer in Figure 3 which will be described below. On the STO substrate, the 500 °C and 800 °C depositions correspond very well to their LAO counterparts in Figure 2 but the 650 °C deposition appeared very vicinal after annealing, indicating an increased response to the miscut of the substrate. The roughness of the films in the right panels of Figure 2 is 6Å (800 °C), 11Å (650 °C), and 25Å (500 °C).

The only AFM evidence for substrate-induced strain is in differences between the 500 °C

Table I. Lattice parameters along the growth direction as obtained from X-ray diffraction. Error in last digit is shown in parenthesis.

Deposition Temp.	SrTiO3 substrate - 3.906 Å		LaAlO3 substrate - 3.791 Å	
	As-deposited	Annealed	As-deposited	Annealed
800 °C	3.885(1) Å	3.867(1) Å	3.915(1) Å	3.882(4) Å
650 °C	3.853(1) Å	3.855(1) Å	3.924(1) Å	3.879(1) Å
500 °C	3.871(1) Å	3.862(3) Å	3.868(2) Å	3.868(1) Å

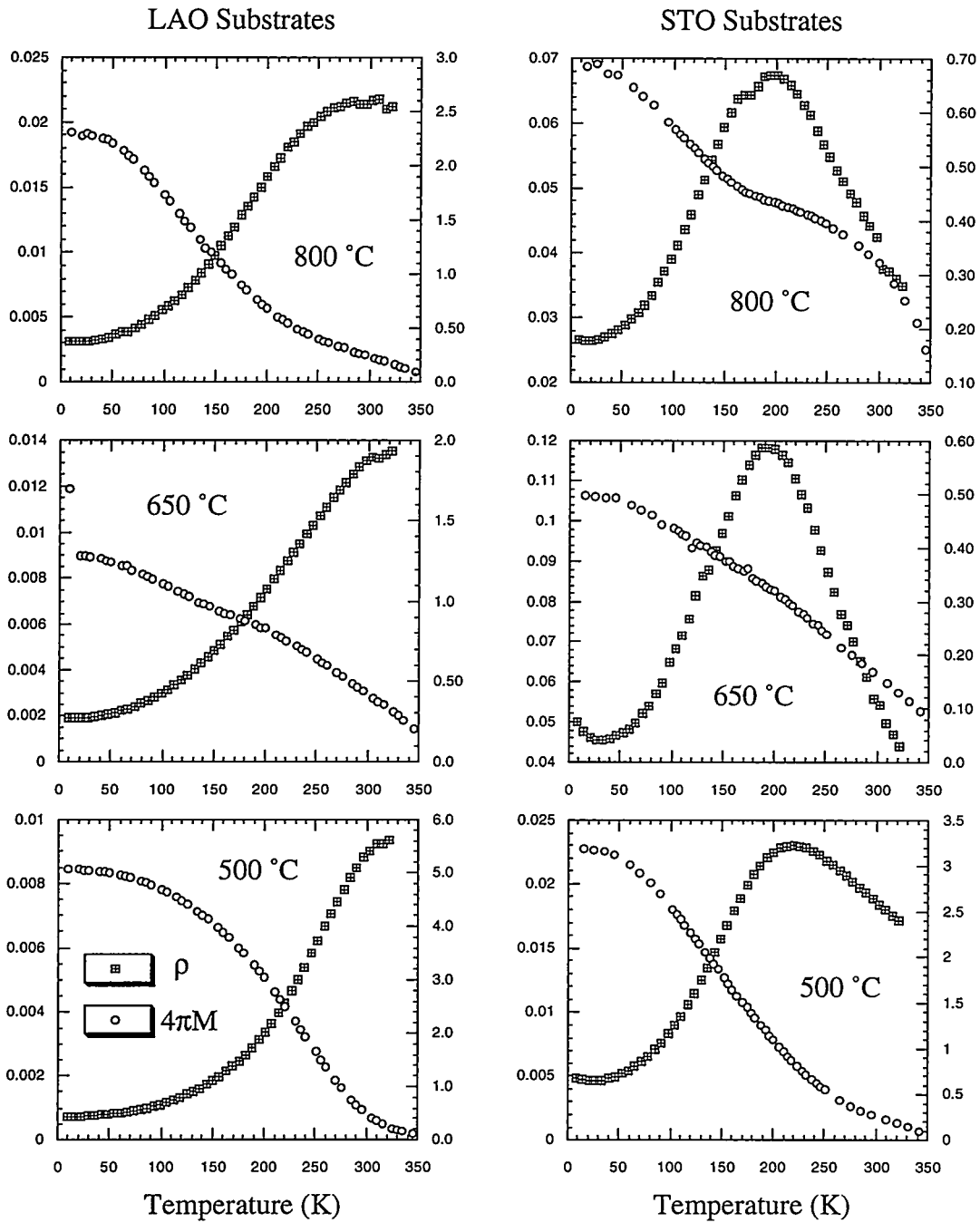


Figure 1. Resistivity and magnetization of annealed LSMO films. Plots show ρ (resistivity in ohm-cm) on left axis and $4\pi M$ (magnetization in kG) on right axis, both as function of temperature. Left panels show films deposited on LAO substrates at temperatures noted while right panels show corresponding depositions on STO. Note that all vertical scales are different to enhance visibility of individual curves.

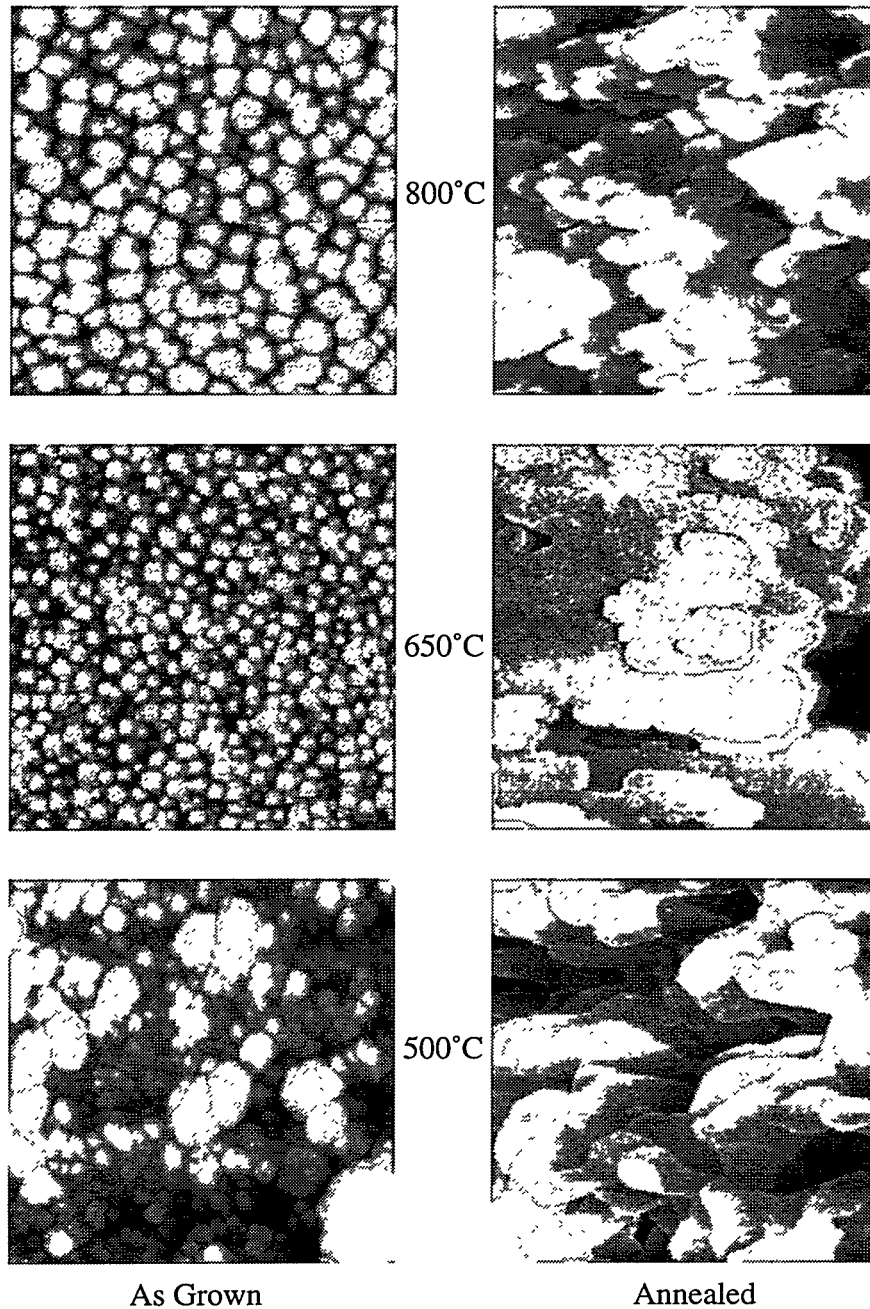


Figure 2. Left panels are $(500 \text{ nm})^2$ images of LSMO as deposited on LAO at the temperatures noted. Right panels are $(500 \text{ nm})^2$ images of annealed LSMO films deposited on LAO simultaneously with the left panel samples. All images are STM data except for the lower left which is AFM data. Roughnesses and grain sizes are noted in text.

films. Panels a) and b) of Figure 3 show $(10\mu\text{m})^2$ scan frames of the annealed 500 °C films on LAO and STO respectively. The STO based LSMO shows a much larger void density, a result which should be stress-related since both LAO and STO based films had lattice constants very nearly equal to each other and the bulk value.

MFM images from some of the as-deposited films appeared to reflect the surface grain structure, but it was not possible to rule out electrostatic and topographic effects that may also contribute to the MFM images under certain conditions. Therefore, no obvious magnetic structure was observed on the as-deposited films. The situation is clearer for the annealed films however. Panel c) is the MFM image of panel b) and shows the voids very clearly but with different strengths than would be implied by their actual depths in panel b), indicating that the image does have magnetic origins. At higher temperatures, there is very obvious magnetic structure. Panel d) shows a $(10\mu\text{m})^2$ scan of the 650 °C deposition on LAO and panel e) shows the corresponding MFM image. Obviously the large magnetic regions do not correspond to anything of comparable size in the topography. The $(1.5\mu\text{m})^2$ AFM and MFM panels, f) and g) respectively, reveal the source of the magnetic signatures. Apparently some of the large magnetic signatures correspond to the surface pinholes that were noted earlier while others likely indicate subsurface pinholes since the magnetic signature is so similar. Weaker signatures imply the existence of even deeper voids. On the 800 °C films, the same signatures exist and appear to be weaker although the data set is still too small to justify comparison of MFM images acquired with different probe tips. Such an effect would be expected on the high temperature depositions since they should be able to more efficiently accommodate stress.

CONCLUSIONS

Pulsed laser deposition was used to produce LSMO over a wide range of temperatures that was epitaxial in the growth direction. Grains increase in size with increasing deposition temperature and then coalesce into terraces with pinholes and screw dislocations upon annealing. Most higher-temperature depositions showed the expected substrate-dependent strain in X-ray-derived lattice constants but the low temperature depositions appeared to have relieved their stress through formation of large voids. No correlations between film morphology and transport or magnetization were evident, indicating that these particular films may have been strongly influenced by strain and/or defects at the growth interface that are not obvious at the surface.

Magnetic structure associated with the pinhole and void defects was observed with MFM. The magnetic signatures associated with the observed pinholes also imply the existence of subsurface voids of similar size and the possibility of detecting them with MFM. The general magnetic domain structure of the films was not obvious in MFM. This is likely the result of imaging above the films' critical temperatures, which came out lower than expected. Since the film stoichiometry and epitaxy was acceptable, these low critical temperatures may also be related to strain at the growth interface. Transmission electron microscopy experiments would be one way to address this issue in future studies.

REFERENCES

1. A. Urushibara, Y. Moritomo, T. Arima, A. Asamitsu, G. Kido, and Y. Tokura, *Phys. Rev. B* **51**, 14103 (1995).
2. Y.-F. Chen, L. Sun, Y. Pan, Y. Tao, Z.-G. Liu, and N.-B. Ming, *Materials Letters* **27**, 139 (1996).
3. H. L. Ju, C. Kwon, Q. Li, R. L. Greene, and T. Venkatesan, *Appl. Phys. Lett.* **65**, 2108 (1994).
4. K. Babcock, M. Dugas, S. Manalis, and V. Eilings, *Proceedings of the Materials Research Society*, **355**, 311 (1995).
5. M.E. Hawley, C.D. Adams, P.N. Arendt, E.L. Brosha, F.H. Garzon, R.J. Houlton, M.F. Hundley, R.H. Heffner, Q.X. Jia, J. Neumeier, and X.D. Wu, to appear in *J. Crystal Growth* **175** (1997).

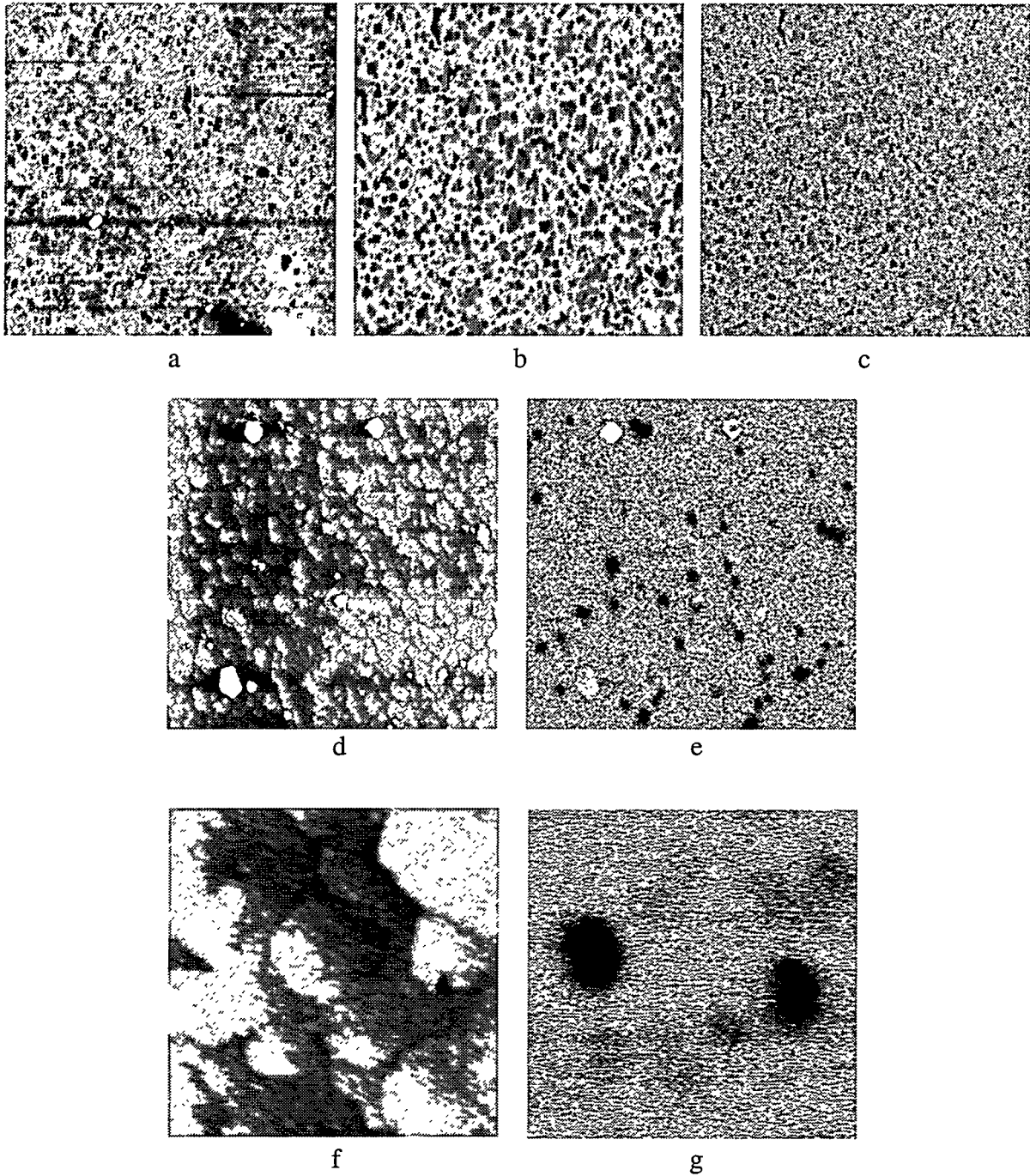


Figure 3. a) 10 μm AFM image of LSMO deposited on LAO at 500 $^{\circ}\text{C}$ and annealed; b) 10 μm AFM image of LSMO deposited on STO at 500 $^{\circ}\text{C}$ and annealed; c) MFM image of area in panel b; d) 10 μm AFM image of LSMO deposited on LAO at 650 $^{\circ}\text{C}$ and annealed; e) MFM image of area in panel d; f) 1.5 μm AFM image of film in panel d; g) MFM image of area in panel f.